Observations of First-Order Liquid-to-Hexatic and Hexatic-to-Solid Phase Transitions in a Confined Colloid Suspension

Andrew H. Marcus and Stuart A. Rice

The James Franck Institute, The University of Chicago, Chicago, Illinois 60637
(Received 8 April 1996)

We have used digital video microscopy to study the equilibrium structure of quasi-two-dimensional suspensions of sterically stabilized uncharged polymethylmethacrylate spheres. Our experiments reveal the existence of an equilibrium hexatic phase as well as strongly first-order liquid-to-hexatic and hexatic-to-solid phase transitions. These observations are in agreement with the predictions of Bladon and Frenkel [Phys. Rev. Lett. **74**, 2519 (1995)] for a confined colloid suspension in which the pair interaction potential between particles has a hard core and either a very short range attraction or a very short range step repulsion. [S0031-9007(96)01052-6]

Two dimensional melting is of great theoretical interest because the type of order that distinguishes the solid from the liquid phase is qualitatively different from that in three dimensions [1]. In the three-dimensional case, the density-density correlation function of the ordered solid phase decays, with increasing particle separation, to a nonzero constant value in the limit of infinite separation. This is the characteristic feature of long-range positional order. In the two dimensional case, the density-density correlation function of the solid phase decays to zero algebraically in the limit of infinite separation, which is the characteristic feature of quasi-long-range order. There is, in a two-dimensional system, a special kind of long-range order called bond orientational order. According to the Kosterlitz-Thouless-Halperin-Nelson-Young (KTHNY) theory [1–5], two-dimensional solids melt via successive dislocation unbinding and disclination unbinding transitions. The first transition is from the solid with quasi-long-range positional order and long-range bond orientation order to a phase with short range positional order and quasi-long-range bond orientational order, the so called hexatic phase. The second transition transforms the hexatic phase to the liquid phase in which both positional and bond orientational order have short range. To date, both experimental and computer simulation studies of two-dimensional melting have focused attention, almost exclusively, on the search for continuous transitions from the solid to the hexatic phase and from the hexatic phase to the liquid phase [6–22]. However, other pathways for two-dimensional melting can occur.

Bladon and Frenkel [12] have reported the results of simulations of a two dimensional assembly of particles which interact via a pairwise additive potential consisting of a hard core repulsion and a very narrow square well attraction. When the width of the well is less than 8% of the diameter, the system supports two ordered solid phases with the same packing symmetry. The locus of the solid-solid transition line ends at a critical point, near which critical point density fluctuations render the solid

unstable with respect to dislocation unbinding, and the system supports a hexatic phase. For the case that the square well width is close to the limiting value for which the low density solid phase becomes unstable, the hexatic region can extend to the melting line. When this occurs the liquid-to-hexatic transition is predicted to be first order while the hexatic-to-solid transition may be either first or second order. The KTHNY theory has been extended, by Chou and Nelson [23], to account for the essential features of the phase diagram found by Bladon and Frenkel.

This Letter reports the results of studies of the structures and phase transitions in a suspension of uncharged colloidal spheres in a very thin cell. The particular system we have studied is a suspension of 0.928 μm diameter spheres of poly(methylmethacrylate) (PMMA). The surface of each PMMA particle was covered with a $\sim$300 Å oligomeric brush of poly(12-hydroxystearic acid) that acts to sterically stabilize it with respect to aggregation. The PMMA particles were suspended in an aqueous sucrose solution (10% by weight) to eliminate sedimentation. The cell walls were coated with trihydroxyoctadecylsilane, which acts to prevent adsorption of the PMMA particles. The spacing between the parallel cell walls was estimated to be approximately 1.2 particle diameters. The properties of these geometrically confined suspensions were studied over the reduced two-dimensional density range $\rho^* = \rho\sigma^2 = 0.01-0.93$, with $\sigma = 0.928$ μm the colloid particle diameter. Further details concerning the sample cell, the digital video microscopy apparatus, and the methods used for data analysis can be found in our previous paper [24].

A key element in the study of two dimensional freezing is the establishment of equilibrium. In the system we studied, it was possible to prepare uniform monolayer suspensions with more than 15 000 particles in the field of view. Consistently reproducible results were achieved by recording data over a 72 h period for each sample density. That there is sufficient time for the system to reach equilibrium is verified by a Voroni polygon analysis of our data, which shows that dislocations and clusters

of dislocations appear and disappear on the time scale of successive video frames (33 ms).

Figure 1 displays Voronoi constructions of sample configurations of PMMA spheres at six densities: $\rho^* = 0.58$, 0.69, 0.83, 0.86, 0.88, and 0.93. Proceeding from the lowest to the highest density, these figures show the system in (A) the pure liquid state, (B) a state with coexistence between liquid and hexatic phases, (C) the pure hexatic phase, (D) a state with coexistence between hexatic and solid, (E) the solid close to the hexatic-solid transition, and (F) a compressed solid. The color scheme employed in Fig. 1 serves to illustrate the observed coexistence displayed in Figs. 1(B) and 1(D), and is based on an analysis of the local bond orientational order parameter, defined as $\psi_6(r_i) = \langle N^{-1} \sum_j \exp\{6i\theta(r_{ij})\}\rangle$ where the index j counts the ith particle's nearest neighbors, $\theta(r_{ij})$ is the angle between the bond connecting particles, j is an arbitrary fixed reference axis, and N is the number of i-j bonds. We have computed the

absolute value of the projection of $\psi_6(r_i)$ onto a local average of the same function over nearest neighbors and next nearest neighbors, namely, $\langle \psi_6^*(r_i) \langle \psi_6(r_i)\rangle_{nn}\rangle^{1/2}$, where the subscript nn refers to the neighbor average. The distribution of this local correlation function is bimodal for configurations exhibiting coexistence, while nearly single mode distributions were obtained for sample configurations of pure phases. The coexisting liquid and hexatic phase densities are 0.68 and 0.70, respectively, while the corresponding coexisting hexatic and solid phase densities are 0.83 and 0.87, respectively. In some cases cells prepared with a colloid density in the liquid-hexatic or hexatic-solid coexistence regions displayed long interfaces between the phases; in other cases the two phases were present as a mixture of small islands.

The identities of the pure phases were established by computing the relevant static correlation functions from statistical averages of the particle positions. We show in Fig. 2 the two dimensional structure functions corre-
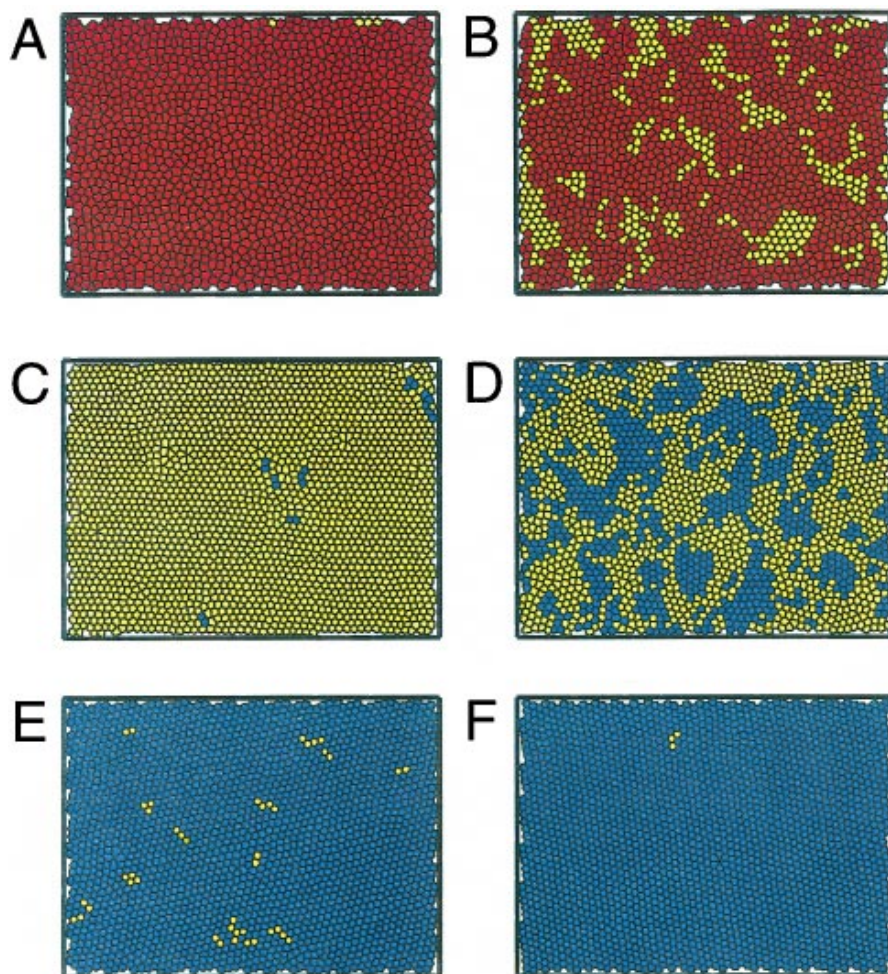

FIG. 1(color). Voronoi constructions of sample configurations of the quasi-two-dimensional assembly of PMMA spheres. Each frame represents an equilibrium state of the system: (A) the pure liquid state, $\rho^* = 0.58$; (B) a state with coexistence between liquid and hexatic phases, $\rho^* = 0.69$; (C) the pure hexatic phase, $\rho^* = 0.83$; (D) a state with coexistence between hexatic and solid, $\rho^* = 0.86$; (E) the solid close to melting, $\rho^* = 0.88$; and (F) a compressed solid, $\rho^* = 0.93$. The color scheme serves to illustrate the observed coexistence displayed in panels (B) and (D), and is based on an analysis of the local bond orientational order parameter described in the text.
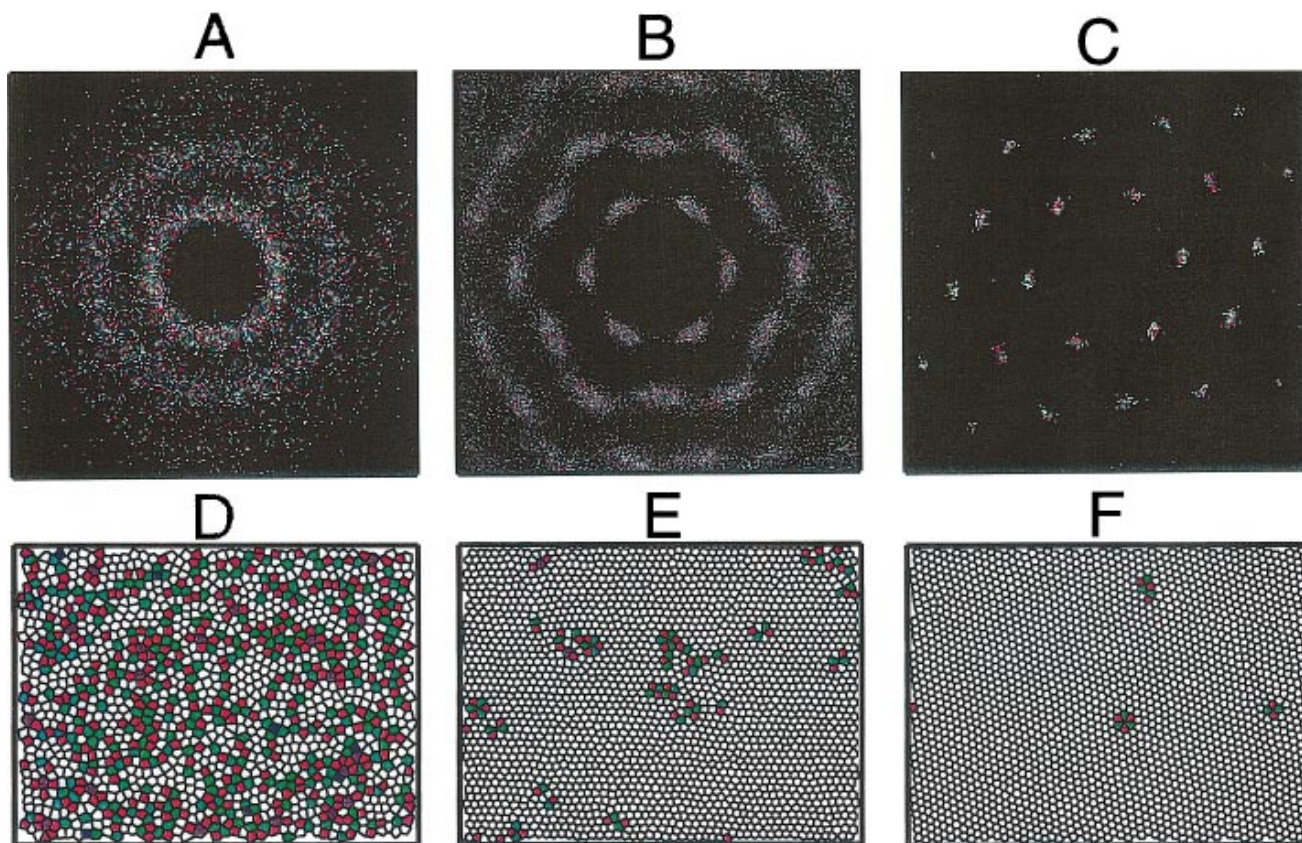
FIG. 2(color).   Computed two dimensional structure functions corresponding to (A) the pure liquid state, $\rho^* = 0.58$; (B) the pure hexatic phase, $\rho^* = 0.83$; and (C) a compressed solid, $\rho^* = 0.93$.   Also shown are the Voronoi constructions of sample configurations at the same densities: (D) $\rho^* = 0.58$, (E) $\rho^* = 0.83$, and (C) $\rho^* = 0.93$.   The color coding is as follows.   Sixfold coordinated sites are white, fivefold sites are red, sevenfold sites are green, fourfold sites are blue, and eightfold sites are purple. In panel (F), a vacant particle appears as a circular bound group of three dislocations.

sponding to the same (A) fluid, (B) hexatic, and (C) solid phase densities described in Fig. 1. Also shown are sample Voronoi constructions [(D)–(F)] where the patterns of defects have been included in the color scheme. The concentration of bound dislocation pairs in the pure solid phase close to the solid-hexatic transition is small ($<0.1\%$) so that the dislocation core energy must be larger than the cutoff predicted by Chui [25] ($2.84 k_B T$) to characterize the crossover between strongly and weakly first order transitions. We conclude that this system falls within the regime where the KTHNY theory should be valid.

The sixfold angular symmetry exhibited in Fig. 2(B) is a necessary but not sufficient condition to distinguish this phase as hexatic. Our identification is further supported by the very good fit shown in Fig. 3(B) of the transverse angular dependent line shape of the structure function to a square-root Lorentzian (SRL), $S(\theta_0) = \{[\theta_0 - \chi]^2 + \kappa^2\}^{-1/2}$, where θ_0 is the angular position of the first peak in the static structure function, χ is the in-plane angle that ranges from zero to 2π, and κ is the SRL angular width. The SRL functional form of the line shape has been established as a signature of hexatic order [26]. Also shown in Fig. 3 are the line shapes of (A) the isotropic fluid and (B) the dense solid phase (which is well fit by a simple Lorentzian function).

More evidence for the assignments we have made of the character of the several phases mentioned above is derived from analysis of the respective pair correlation functions (Fig. 4). The translational correlation functions
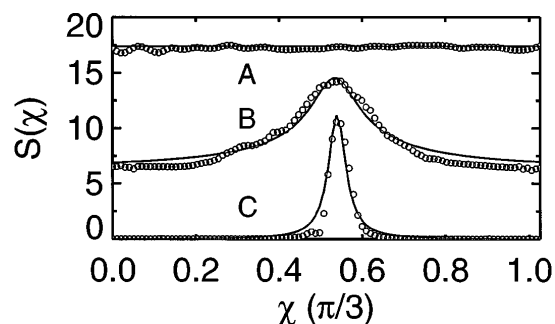

FIG. 3.   Angular dependences of the line shapes of the two dimensional structure functions (evaluated at the wave vector corresponding to the first peak, $|\mathbf{k}_{max}|$) shown in Figs. 2(A)– 2(C). The curves are displaced on the vertical scale for clarity. (A) $k_{max} = 5.2\ \mu\mathrm{m}^{-1}$; there is no angular dependence for the isotropic fluid phase, while the hexatic line shape (B) $k_{max} = 6.2\ \mu\mathrm{m}^{-1}$ agrees very well with a square-root Lorentzian (solid line, $0.48[(\chi - 0.54\ \mathrm{rad})^2 + (0.056\ \mathrm{rad})^2]^{-1/2}$; see text). The solid phase (C) $k_{max} = 6.4\ \mu\mathrm{m}^{-1}$ is well fit by a simple Lorentzian function, $0.007[(\chi - 0.54\ \mathrm{rad})^2 + (0.025\ \mathrm{rad})^2]^{-1}$.
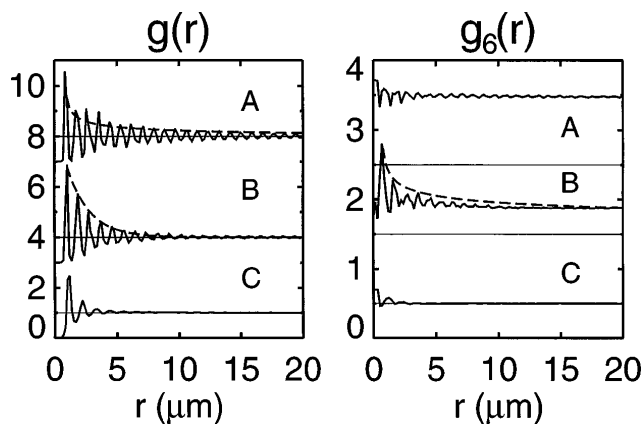
FIG. 4. Translational and bond orientational correlation functions as a function of density. The curves have been shifted vertically for clarity. For both sets of curves, the three pure phases are represented with the same densities as given in the previous figures. The envelope for the compressed solid (A) decays algebraically (dotted curve), while it remains constant. For the hexatic phase (B), decays exponentially $[\sim\exp(-r/(1.8~\mu m))]$, while decays algebraically. In the fluid state (C), both correlation functions decay exponentially.

were obtained by computing histograms of the measured distribution of particle separations. In an analogous fashion, the global bond orientational correlation functions were computed according to the definition [4] $g_6(r) = \langle\psi^*(0)\psi(r)\rangle\langle\delta(\mathbf{r_i})\delta(\mathbf{r_j} - \mathbf{r})\rangle^{-1}$, where the index i runs over all particles, and j counts the ith particle's nearest neighbors.

Within the precision of our data, the positional order in the solid phase is seen to decay with increasing particle separation as $\sim r^{-1/3}$ (dotted curves in Fig. 4), while the angular order does not decay at all. In the hexatic phase we find that the translational order decays exponentially with increasing particle separation as $\sim\exp[-r/(1.8~\mu m)]$, while the angular order decays as $\sim r^{-1/4}$; in the fluid phase both the positional order and the angular order decay exponentially with increasing particle separation.

These are, to our knowledge, the first observations of strongly first order fluid-to-hexatic and hexatic-to-solid phase transitions in a physically realized experimental quasi-two-dimensional system. We note that our particles differ from those used in previous investigations [18–21] in that they are electrically neutral. Our findings are consistent with the model proposed by Bladon and Frenkel [12]. In the system we have studied, the short range potential between colloid particles is associated with the extent of the stabilizing oligomeric brush coating the particle surfaces. Although the surface density and the extent of elongation of the brush away from the surface are not precisely known, the contour length of the brush (~300 Å) does fall within the expected interaction range for the behavior predicted by Bladon and Frenkel. A study of the

nature of the interparticle potential will be presented in our forthcoming paper [27].

[1] For a review, see D. R. Nelson, in *Phase Transitions and Critical Phenomena,* edited by C. Domb and J. L. Leibowitz (Academic Press, London, 1983), Vol. 7.

[2] J. M. Kosterlitz and D. J. Thouless, J. Phys. **C5**, L124 (1972); **C6**, 1181 (1973).

[3] B. I. Halperin and D. R. Nelson, Phys. Rev. Lett. **41**, 121 (1978).

[4] D. R. Nelson and B. I. Halperin, Phys. Rev. B **19**, 2457 (1979).

[5] A. P. Young, Phys. Rev. B **19**, 1855 (1979).

[6] V. M. Bedanov, G. V. Gadiyak, and Y. E. Lozovik, Phys. Lett. **92A**, 400 (1982).

[7] V. M. Bedanov, G. V. Gadiyak, and Y. E. Lozovik, Sov. Phys. JETP **61**, 967 (1985).

[8] K. J. Naidoo and J. Schnitker, J. Chem. Phys. **100**, 3114 (1994).

[9] H. Weber, D. Marx, and K. Binder, Phys. Rev. B **51**, 14 636 (1995).

[10] K. Bagchi, H. C. Anderson, and W. Swope, Phys. Rev. Lett. **76**, 255 (1996).

[11] M. A. Stan and A. J. Dahm, Phys. Rev. B **40**, 8995 (1989).

[12] P. Bladon and D. Frenkel, Phys. Rev. Lett. **74**, 2519 (1995).

[13] For a review, see C. A. Murray, in *Bond Orientational Order in Condensed Matter Systems,* edited by K. J. Strandberg (Springer-Verlag, New York, 1992).

[14] T. Keyes and B. Ladanyi, J. Chem. Phys. **62**, 4787 (1975).

[15] G. Deville, A. Valdes, E. Y. Andrei, and F. I. B. Williams, Phys. Rev. Lett. **54**, 1710 (1985).

[16] D. C. Glattli, E. Y. Andrei, and F. I. B. Williams, Phys. Rev. Lett. **60**, 420 (1988).

[17] H. W. Jiang and A. J. Dahm, Surf. Sci. **229**, 352 (1990).

[18] C. A. Murray and D. H. Van Winkle, Rev. Lett. **58**, 1200 (1988).

[19] C. A. Murray and R. A. Wenk, Phys. Lett. **62**, 1643 (1989).

[20] C. A. Murray, W. O. Sprenger, and R. A. Wenk, Phys. Rev. B **42**, 688 (1990).

[21] A. J. Armstrong, R. C. Mockler, and W. J. O'Sullivan, J. Phys. Condens. Matter **1**, 1707 (1989).

[22] For a review, see K. J. Strandberg, Rev. Mod. Phys. **60**, 161 (1988).

[23] T. Chou and D. R. Nelson, Phys. Rev. E **53**, 2560 (1996).

[24] A. Marcus, B. Lin, and S. A. Rice, Phys. Rev. E (to be published).

[25] S. T. Chui, Phys. Rev. B **28**, 178 (1973).

[26] S. C. Davey, J. Budai, J. W. Goodby, R. Pindak, and D. E. Moncton, Phys. Rev. Lett. **53**, 2129 (1984); G. Aeppli and R. Bruinsma, Phys. Rev. Lett. **53**, 2133 (1984).

[27] A. H. Marcus and S. A. Rice (to be published).